

Published in final edited form as:

Nat Cell Biol. 2006 August ; 8(8): 877–884. doi:10.1038/ncb1448.

Plasminogen activator inhibitor-1 is a critical downstream target of p53 in the induction of replicative senescence

Roderik M. Kortlever¹, Paul J. Higgins², and René Bernards^{1,3}

¹Division of Molecular Carcinogenesis and Center for Biomedical Genetics, The Netherlands Cancer Institute, Plesmanlaan 1211066 CX Amsterdam, The Netherlands. ²Center for Cell Biology & Cancer Research, Albany Medical College, MC-165, 47 New Scotland Avenue, Albany, NY 12208, USA.

Abstract

p53 limits the proliferation of primary diploid fibroblasts by inducing a state of growth arrest named replicative senescence — a process which protects against oncogenic transformation and requires integrity of the p53 tumour suppressor pathway^{1–3}. However, little is known about the downstream target genes of p53 in this growth-limiting response. Here, we report that suppression of the p53 target gene encoding plasminogen activator inhibitor-1 (*PAI-1*) by RNA interference (RNAi) leads to escape from replicative senescence both in primary mouse embryo fibroblasts and primary human BJ fibroblasts. *PAI-1* knockdown results in sustained activation of the PI(3)K–PKB–GSK3 β pathway and nuclear retention of cyclin D1, consistent with a role for PAI-1 in regulating growth factor signalling. In agreement with this, we find that the PI(3)K–PKB–GSK3 β –cyclin D1 pathway is also causally involved in cellular senescence. Conversely, ectopic expression of PAI-1 in proliferating p53-deficient murine or human fibroblasts induces a phenotype displaying all the hallmarks of replicative senescence. Our data indicate that PAI-1 is not merely a marker of senescence, but is both necessary and sufficient for the induction of replicative senescence downstream of p53.

Primary murine fibroblasts activate the p19^{ARF}–p53 tumour suppressor pathway during prolonged culturing *in vitro*, which induces a post-mitotic state referred to as replicative senescence. Senescence can be overcome by loss of either p19^{ARF}, p53 or the combined loss of all three retinoblastoma family proteins^{1,2}. Proliferation of fibroblasts is induced by growth factors which activate cyclin-dependent kinases (CDKs), and in turn inactivate pRb's growth-limiting ability², a G1 cell-cycle checkpoint that is often deregulated in cancer³. It is unclear which of the many downstream p53-target genes is responsible for the p53-dependent induction of replicative senescence. An attractive candidate is the CDK inhibitor *p21^{CIP1}*. However, mouse embryo fibroblasts (MEFs) knocked out for *p21^{CIP1}* are not immortal⁴.

Here, we identify an unexpected causal role for the urokinase type plasminogen activator (uPA)–PAI-1 system in the induction of replicative senescence. The serpin and extra-cellular matrix (ECM)-associated protein PAI-1 is a direct target of p53 (ref. ^{5, 6}), is upregulated in

³Correspondence should be addressed to R.B. (r.bernards@nki.nl).

AUTHOR CONTRIBUTIONS

R.K. and R.B. conceived and designed the experiments. R.K. performed the experiments. P.H. contributed materials. R.K. and R.B. analysed the data. R.K. and R.B. wrote the paper.

COMPETING FINANCIAL INTERESTS

The authors declare that they have no competing financial interests.

Note: Supplementary Information is available on the Nature Cell Biology website.

ageing fibroblasts *in vivo* and *in vitro*, and is considered a marker of replicative senescence^{7–9}. PAI-1 inhibits the activity of the secreted protease uPA by forming a stable complex. uPA expression can cause cells to progress through G1 into S phase¹⁰, most likely through activating a mitogenic signalling cascade by increasing the bioavailability of growth factors.

To investigate the role of PAI-1 in replicative senescence, two independent retroviral vectors were generated that targeted murine *PAI-1* for suppression through RNAi¹¹. When primary MEFs were infected with either *PAI-1* knockdown (kd) construct (*PAI-1^{kdI}* or *PAI-1^{kdII}*), bypass of senescence was observed in a colony formation assay (Fig. 1a). As inhibition of *PAI-1* expression leads to activation of uPA^{12,13}, we asked whether overexpression of uPA also caused immortalisation. Retrovirus-mediated over-expression of pro-uPA was as efficient as *PAI-1* knockdown in causing immortalisation of MEFs (Fig. 1a). To assess *PAI-1* levels in infected MEFs, *p53^{kd}*, *PAI-1^{kd}* or *uPA* overexpressing cells were serially passaged until they had become post-senescent at passage 9 (P9) (that is, when control MEFs were senescent) and observed a significant reduction in *PAI-1* mRNA expression in *PAI-1^{kd}* MEFs by quantitative RT-PCR (QRT-PCR; Fig. 1b). As *PAI-1* is a transcriptional p53 target^{5,6} and p53 is activated during replicative senescence, *PAI-1* is highly expressed in senescent MEFs⁹. Accordingly, P9 MEFs expressed more *PAI-1* than P3 or *p53^{kd}* cells, which had comparable *PAI-1* mRNA levels (Fig. 1b). uPA activity is downstream of PAI-1 and p53, and consequently immortal cells overexpressing uPA have *PAI-1* expression levels similar to those observed in P9 MEFs (Fig. 1b). When examined in a long-term cell proliferation assay, *PAI-1^{kd}* also extended the proliferative capacity of MEFs far beyond that of wild-type cells (see Supplementary Information, Fig. S1a). Spontaneous immortalisation of MEFs can be caused either by mutation of p53 or by loss of p19^{ARF} expression^{14–16}, which was not observed in *PAI-1^{kd}* cells as judged by their normal p53-dependent DNA-damage response (see Supplementary Information, Fig. S1b). As p19^{ARF} levels in *PAI-1^{kd}* cells are comparable with those observed in wild-type senescent cells, we concluded that p19^{ARF} expression is not lost after knockdown of *PAI-1*. Consistent with these observations, *PAI-1* knockout (*PAI-1^{-/-}*) MEFs proliferated well beyond the senescence checkpoint, albeit at a slower rate than *p53^{-/-}* MEFs (Fig. 1c). Importantly, six independent immortal *PAI-1^{-/-}* MEF cell lines showed normal p53 function after DNA-damage exposure (Fig. 1d).

Next, we sought to understand the molecular pathway(s) involved in the immortalisation of MEFs after *PAI-1* knockdown or uPA overexpression. The tumour suppressors p16^{INK4A} and p21^{CIP1} were induced in P9 MEFs and immortal *PAI-1^{kd}* or uPA overexpressing cells, indicating that the senescence-stress pathway is activated in these MEFs (Fig. 2a). Interestingly, a sharp increase in cyclin D1 levels were observed in both non-proliferating P9 and proliferating *PAI-1^{kd}* or uPA overexpressing MEFs, which may neutralize the high levels of p21^{CIP1} (Fig. 2a). We asked whether signalling through PI(3)K, PKB (also known as AKT) and GSK3 β was involved. Activation of PI(3)K and subsequent full activation of PKB by phosphorylation on Ser 473 leads to an inhibitory phosphorylation of GSK3 β on Ser 9 by PKB^{17,18}. GSK3 β controls cyclin D1 localization and degradation through an inhibitory phosphorylation on Thr 286 and loss of this inhibitory phosphorylation protects cyclin D1 from nuclear exclusion and degradation¹⁹. Therefore, mitogenic signalling through PI(3)K–PKB–GSK3 β influences cyclin D1 stability and its nuclear activity, leading to cell-cycle progression². uPA induces growth factor-related PI(3)K–PKB signalling²⁰ and, as a result, uPA activity may result in nuclear retention of cyclin D1 by inducing loss of GSK3 β activity through phosphorylation on Ser 9. When cyclin D1 localization was determined in ageing MEFs, a striking but gradual nuclear exclusion of cyclin D1 was observed (Fig. 2b), which correlated with the decline in growth rate (note that wild-type MEFs became fully senescent at passage 8; see Supplementary Information, Fig. S2a, as confirmed by staining for senescence-associated acidic β -galactosidase²¹, SA- β -Gal; data not shown). Furthermore, during serial passaging, wild-type MEFs show a progressive decline in PKB activation by loss

of phosphorylation and a gradually increased GSK3 β activation by loss of inhibitory phosphorylation (Fig. 2c). In contrast, immortal PAI-1^{kd} or uPA overexpressing MEFs had sustained PKB–GSK3 β signalling (see Supplementary Information, Fig. S2b). We therefore concluded that during replicative senescence cyclin D1 is excluded from the nucleus and stabilized in the cytosol, correlating with decreased growth-rate and downregulation of PKB–GSK3 β signalling. The high levels of cyclin D1 found in senescent cells (Fig. 2a) were unexpected because GSK3 β activity induces not only nuclear exclusion, but also the turnover of cyclin D1 (ref. ¹⁹). Significantly, high levels of cyclin D1 were also observed in senescent human BJ fibroblasts (Fig. 5c). Apparently, the turnover of cyclin D1 is different in senescent cells as compared with cycling NIH3T3 cells¹⁹.

We next examined whether immortalisation of MEFs by *PAI-1* knockdown may be the result of activated PI(3)K–PKB–GSK3 β signalling. Primary MEFs were retrovirally transduced with constitutively active mutants of PI(3)K (p110 α ^{CAAX}; Ca-PI(3)K) or PKB (Myr-PKB; Ca-PKB), a retroviral knockdown short hairpin RNA (shRNA) construct for GSK3 β , or retroviral expression constructs for wild-type cyclin D1 (D1) or non-degradable cyclin D1 (T286A-cyclin D1; TA-D1), and determined their immortalizing potential in a colony-formation assay. The TA-D1 mutant is refractory to phosphorylation by GSK3 β and is therefore constitutively nuclear¹⁹. We found that Ca-PI(3)K, Ca-PKB, GSK3 β ^{kd} or TA-D1 (but not wild type D1) are individually capable of immortalizing wild-type MEFs (Fig. 3a). Furthermore, no loss of p19^{ARF} expression or evidence for mutation of p53 was found in any of the immortalised MEFs (data not shown). When tested in a long-term proliferation assay, overexpression of Ca-PI(3)K, Ca-PKB, GSK3 β ^{kd} or TA-D1 (but not wild type D1) also induced a bypass of senescence in MEFs (Fig. 3b). Again, immortalisation was not accompanied by loss of p19^{ARF} or p53 function (data not shown). As previously observed in PAI-1^{kd} or uPA overexpressing MEFs (Fig. 2a), induction of p21^{CIP1} protein levels in the post-senescent polyclonal cell lines expressing a Ca-PI(3)K, Ca-PKB, GSK3 β ^{kd}, or TA-D1 construct was noted (see Supplementary Information, Fig. S2c). Furthermore, high PKB-GSK3 β signalling was observed in Ca-PI(3)K or Ca-PKB overexpressing cells and reduced GSK3 β expression in GSK3 β ^{kd} cells (see Supplementary Information, Fig. S2d). Our results suggest that enforced constitutive activation of PI(3)K–PKB signalling, reduction of GSK3 β activity or nuclear retention of cyclin D1, is sufficient to bypass senescence in MEFs downstream of p53. Accordingly, immunofluorescence microscopy analysis of post-senescent polyclonal cell lines of MEFs immortalised with the various constructs used in this study revealed nuclear localization of endogenous cyclin D1 when compared with senescent wild-type or HA-tagged cyclin D1 expressing MEFs (Fig. 3c and see Supplementary Information, Fig. S2e).

To examine whether reduction of PI(3)K–PKB–GSK3 β signalling is sufficient for the induction of senescence, antagonists of this mitogenic signalling route were overexpressed in *p53*-depleted cells. Retroviral cDNA expression constructs were generated for human *PAI-1* (which is not targeted by the mouse PAI-1^{kd} vectors), mouse *PTEN* and *GSK3 β* . PTEN is a potent tumour suppressor often deleted in cancer that blocks the activation of PI(3)K²² and exerts its effect in part by regulating nuclear availability of cyclin D1 (ref. ²³). When overexpressed in *p53*^{kd} or *PAI-1*^{kd} cells, PAI-1, PTEN and GSK3 β were all individually able to induce senescence, as observed by a flat-cell morphology and positive staining for SA- β -Gal. (Fig. 4a–d). To test whether cyclin D1 is an essential target downstream of PAI-1, PAI-1 was overexpressed in *p53*^{-/-} MEFs, MEFs overexpressing TA-D1, or pocket-protein deficient triple knockout cells (pRb^{-/-}-p107^{-/-}-p130^{-/-}; TKO). The immortal TKO controls lack retinoblastoma family function and therefore have sustained E2F activity^{24,25}. In normal fibroblasts pRb (family)-E2F-mediated repression is required for cell-cycle exit in response to p19^{ARF}-p53 activation²⁶. Overexpression of TA-D1 in MEFs may therefore resemble the phenotype seen in TKO cells by blocking retinoblastoma family function. Figure 4e shows that PAI-1 induced an arrest in *p53*^{-/-} cells, but not when these cells also expressed TA-D1 or were

pocket-protein deficient. These results suggest that in the presence of a wild-type cyclin D1 protein, PAI-1 is able to induce an arrest, but not when cyclin D1 is constitutively nuclear and insensitive to GSK3 β .

The senescence response of human fibroblasts is, in the first instance, primarily dependent on p53 (M1 checkpoint) and, as in MEFs, PAI-1 is upregulated during ageing and is a marker of senescence in these cells^{7,27}. When primary human BJ fibroblasts were infected with either one of two independent human-specific *PAI-1* knockdown constructs (*PAI-1*^{kd} I or *PAI-1*^{kd} II) an M1 senescence-bypass was observed as judged in a long-term growth assay (Fig. 5a). As in MEFs, overexpression of uPA also induced a bypass of senescence in primary BJ cells, albeit with lower efficiency (Fig. 5a). When the post-senescent and proliferating population doubling (PD) 68 *PAI-1*^{kd} were assayed for *PAI-1* levels, reduction to levels even below those observed in young PD 30 BJ fibroblasts was observed (Fig. 5b). *PAI-1* levels in PD 68 uPA overexpressing BJ cells were similar to those seen in senescent cells, in agreement with the notion that uPA acts downstream of p53. *PAI-1*^{kd} or uPA overexpressing fibroblasts have notably higher levels of *p21*^{CIP1} than p53^{kd} cells (Fig. 5b, c), consistent with the notion that *PAI-1*^{kd} mediates senescence-bypass downstream of p53. That p53 is wild type in the *PAI-1*^{kd} or uPA over-expressing BJ fibroblast is also supported by their normal response to DNA damage (data not shown). As observed in MEFs, induction of cyclin D1 in *PAI-1*^{kd} and uPA overexpressing post-senescent BJ cells, as well as in non-proliferating senescent BJ cells, was observed (Fig. 5c). Furthermore, an increase in cytoplasmic cyclin D1 in ageing BJ fibroblasts was noticed, which was associated with p21^{CIP1} (see Supplementary Information, Fig. S4a–c), although the nuclear-to-cytoplasmic transition of cyclin D1 seems to be not as pronounced as in ageing MEFs. Importantly, overexpression of murine PAI-1, PTEN, or GSK3 β in immortal human p53^{kd} or *PAI-1*^{kd} cells induced an arrest and SA- β -Gal. staining (Fig. 5d, e), indicating that PAI-1 expression and downregulation of the PI(3)K–PKB–GSK3 β signalling route are also sufficient for induction of senescence in human fibroblasts downstream of p53 and PAI-1. Taken together, we conclude that PAI-1 is necessary and sufficient for senescence in human BJ fibroblasts. As *p21*^{CIP1} is an essential p53 target in the senescence response of human fibroblasts^{28,29}, we asked if simultaneous knockdown of both *p21*^{CIP1} and PAI-1 would induce a more efficient bypass of senescence than either one alone. Knockdown of the expression of either *PAI-1* or *p21*^{CIP1} resulted in a less efficient senescence-bypass than observed with knockdown of *p53* (see Supplementary Information, Fig. 5a, b). Interestingly, simultaneous knockdown of *PAI-1* and *p21*^{CIP1} resulted in a more efficient bypass of the arrest than knockdown of *p53* itself (see Supplementary Information, Fig. S5a–c). We conclude that PAI-1 and *p21*^{CIP1} are both relevant downstream targets of p53 in the induction of senescence in human fibroblasts, as evident from the effects of their combined knockdown.

Here, we show that PAI-1 is a critical downstream target of p53 in the senescence response of both ageing mouse and human diploid fibroblasts. Our data indicate that p53 controls growth factor-dependent proliferation by upregulating PAI-1, leading to down-regulation of PI(3)K–PKB signalling and nuclear exclusion of cyclin D1. Conversely, we found that loss of *PAI-1* expression or uPA overexpression in MEFs conferred resistance to the anti-proliferative activity of p53 by inducing sustained PI(3)K–PKB signalling and cyclin D1 nuclear retention. Our data are consistent with a model in which PAI-1 acts to limit cyclin–CDK activity during the induction of replicative senescence and suggest a role for PAI-1 as a secreted gatekeeper of fibroblast proliferative capacity (Fig. 5f).

We found that the mitogen-stimulated PI(3)K–PKB pathway is causally involved in the senescence-bypass of fibroblasts, and that overexpression of its antagonist, PTEN²², can reverse this process. It has been reported that the levels of PTEN are crucial in determining the senescence response of fibroblasts — partial loss of PTEN confers a proliferative advantage,

whereas acute loss of all PTEN induces senescence³⁰. Consistent with this, we found that somatic knockdown of *PTEN* in wild-type MEFs resulted in bypass of senescence (data not shown) and constitutive activation of the PI(3)K–PKB signalling route, albeit not to the degree seen in Ca-PI(3)K or Ca-PKB overexpressing cells (see Supplementary Information, Fig. S3b). In apparent conflict with our data, which show senescence bypass by active PKB, it has been reported that overexpression of an active PKB resulted in induction of senescence. However, when these cells were followed over 6 days, proliferation was not entirely lost in the infected population³⁰. We have selected PKB-infected wild type MEFs over a longer period of time, and consequently enriched for proliferating cells with potentially only moderately enhanced PKB activity. Taken together, these data support the notion that slightly elevated levels of PKB or partial loss of PTEN results in enhanced proliferation, whereas highly elevated PKB or complete loss of PTEN induces senescence. This is reminiscent of what has been observed in RAS signalling, where overexpression of an activated *RAS* oncogene induces senescence, whereas activated RAS expressed at physiological levels confers a growth advantage³¹.

PAI-1 is induced by a variety of growth factors and is a target of c-Myc^{7,32}. uPA transcription and its extracellular activity are regulated by growth-factor signalling and proteases. Induction of PAI-1 may therefore be part of a growth factor-stimulated negative feedback loop that becomes constitutively activated by p53 in ageing fibroblasts. As a consequence, senescent fibroblasts may induce a state of growth-factor unresponsiveness by secreting PAI-1. It is therefore possible that induction of *PAI-1* by p53 or disturbance of the uPA or PAI-1 levels influences intra-tumour heterotypic signalling and the local tumour microenvironment. This is particularly noteworthy as uPA and PAI-1 are causally involved in wound healing, angiogenesis and metastasis^{12,33} — processes that are dominantly regulated by cell–cell signalling³⁴. Furthermore, uPA is secreted by stromal fibroblasts and myofibroblasts at the invasive front in breast and prostate cancer³⁵ and loss of uPA can result in reduced metastasis in mouse models^{36,37}. As it is becoming increasingly clear that stromal tissue is an indispensable player in neoplastic transformation and metastasis^{38,39}, our observations may lead to a better understanding of the role of fibroblasts in cancer.

METHODS

Antibodies and Vectors

For western blotting, antibodies against p16^{INK4A} (M156), p21^{CIP1} (F5, C19), SP1 (PEP2), cyclin D1 (H295, M20), cyclin E (M20), PCNA (PC-10), PKB–Akt1 (C20), p53 (DO-1), HA (Y11) and CDK4 (C22) were purchased from Santa Cruz Biotechnology (Santa Cruz, CA); anti p-PKB (Ser473; #9271), anti p-GSK3 β (Ser9; #9336) and HSP90 (#4874) from Cell Signalling (Beverly, MA); anti p19^{ARF} (Ab 80-100) from Abcam (Cambridge, UK); anti-GSK3 β (610201) from BD Pharmingen (San Jose, CA); anti phosphotyrosine (PY20) from Calbiochem (San Diego, CA); and anti p53 (Ab7) from Oncogene Research Products (Boston, MA). Flag-tagged mouse cDNAs for *PAI-1*, *GSK3 β* , *PTEN* or human *PAI-1* were generated by PCR amplification and cloned into pLZRS–IRES–zeocin. Mouse cDNA for *uPA* was generated by PCR amplification of pro-uPA and cloned into pBABEpuro. The production of siRNAs in MEFs, BJ or tsLT–hTERT–BJ fibroblasts was achieved using the pRETRO–SUPER vector¹¹. For the generation of mouse *PAI-1* knockdown constructs the following 19-mer sequences were used: PAI-1 I, 5′-GAACAAGAATGAGATCAGT-3′; PAI-1 II, 5′-GTTGGGCATGCCTGACATG-3′. For the generation of human *PAI-1* knockdown constructs the following 19-mer sequences were used: PAI-1 I, 5′-CTGACTTCACGAGTCTTTC-3′; PAI-1 II, 5′-CCTGGGAATGACCGACATG-3′. The 19-mer sequences used for knockdown of mouse *p53* or *GSK3 β* have been described elsewhere^{40,41}, as have the 19-mer sequences used for knockdown of human *p53* or *p21^{CIP1}* (ref. 29). Control infections were performed with nonfunctional hairpin or red fluorescent protein (RFP) vectors.

Cell culture, transfection and retroviral infection

MEFs, primary and tsLT hTERT human BJ fibroblasts and Phoenix cells were cultured in DMEM (Gibco, Carlsbad, CA) supplemented with 8% heat-inactivated fetal bovine serum (Perbo; PAA, Pasching, Austria), 2 mM L-glutamine and penicillin–streptomycin (Gibco). Transfections were performed with the calcium-phosphate precipitation technique. Retroviral supernatants were produced by transfection of Phoenix packaging cells. Viral supernatants were filtered through a 45 µm Millex HA filter (Millipore, Carrigtwohill, Ireland) and infections were performed in the presence of 4 µg ml⁻¹ polybrene (Sigma, St Louis, MO). Drug selections in MEFs or BJs were performed with 1 µg ml⁻¹ puromycin, 50 µg ml⁻¹ hygromycin or 100 µg ml⁻¹ zeocin.

Colony-formation assays

Wild-type MEFs were infected with shRNA or cDNA constructs at P3, selected and at P5 5×10^4 cells were seeded onto 10-cm plates and stained after 3 weeks. p53^{kd} control MEFs (5×10^4) were seeded onto 10-cm plates and stained after 1, 2 or 3 weeks. Immortal *PAI-1^{kd}* MEFs were infected, after 72 h were plated under low density (5×10^4 cells in a 10-cm plate) and 2 weeks were later stained. p53^{-/-}, TA-D1 or TKO MEFs were infected, 48 h after infection 5×10^4 cells were seeded onto 10-cm plates and were stained after 1 week. Human post-senescent p53^{kd} or *PAI-1^{kd}* BJ fibroblasts were infected with cDNA constructs, plated under low density (1×10^5 cells in a 10-cm plate) and were stained after 2 weeks. Human tsLT BJ fibroblasts were infected at 32 °C and after 48 h, 1×10^5 cells were seeded per 10-cm plate, shifted to 39 °C and stained after 2 weeks. For all colony formations representative examples of at least three independent experiments are shown.

Growth curves

MEFs were infected with retroviral shRNA or cDNA expression constructs at P3, selected and at P5 1.5×10^5 cells were plated in a 6-cm dish (time = 0 days). Every 4 days, cells were counted and 1.5×10^5 cells were replated. A MEF passage, as defined for this paper, represents 4 days in culture. *PAI-1^{-/-}*, p53^{-/-} or wild-type MEFs (1.5×10^5) were plated in a 6-cm dish at P1, and every 4 days cells were counted and 1.5×10^5 cells were replated. Human primary BJ fibroblasts at population-doubling 53 were infected, selected and 1.5×10^5 cells were plated in a 6-cm dish (time = 0 days). Every 4 days, cells were counted and 1.5×10^5 cells were replated. Human tsLT BJ fibroblasts were infected, shifted to 39 °C after 48 h and 1.5×10^5 cells were plated in a 6-cm dish (time = 0 days). Every 6 days, cells were counted and 1.5×10^5 cells were replated. The p53 status of control, senescent or post-senescent primary MEFs, BJ fibroblasts or tsLT BJ fibroblasts was checked by DNA-damage induced p53 activation by overnight addition of 0.5 mM cisplatin and western blotting for p53 and its targets (p19^{ARF} and p21^{CIP1} in MEFs, or p21^{CIP1} and Bax in BJ fibroblasts). Total cell amounts in all growth curves were displayed as cumulative over time. For all growth-curves representative examples of at least two independent experiments are shown.

Quantitative RT-PCR

Total RNA from immortal post-senescent MEF cell lines plus P3 and 9 control MEFs, control or immortalized human BJ fibroblasts and immortalised tsLT BJ fibroblasts at 39 °C or controls at 32 °C or 39 °C, was isolated with TRI-Zol (Invitrogen, Carlsbad, CA) according to manufacturers' instructions. QRT-PCR was performed on an ABI Prism 7700 with Assays-on-Demand (Applied Biosystems, Foster City, CA) for mouse *PAI-1* and *TBP* as a control housekeeping gene, or for human *PAI-1* or p21^{CIP1} with *GAPDH* as a control housekeeping gene. QRT-PCR results in tsLT BJ fibroblasts are the mean ± s.d. of three independent cell lines per genotype. For all QRT-PCRs, representative examples of at least two independent experiments are shown.

Immunofluorescence microscopy

Cells were plated on 8-well chamber slides (Nutacon; Leimuiden, The Netherlands) and cultured overnight after which they were fixed with 4% formaldehyde in PBS for 15 min, permeabilized with 0.2% Triton X (Sigma), blocked and incubated with anti-cyclin D1 (M20) from Santa Cruz Biotechnology. Actin was stained with rhodamine-conjugated phalloidin (Invitrogen) and the nucleus with DAPI (Roche, Basel, Switzerland). Images were obtained using a Modified Zeiss Axiovert 100M (SP LSM 5) cooled CCD fluorescence microscope with a Plan-APOCHROMAT, 1.0 NA, 40× oil immersion objective plus a Zeiss single excitation-triple emission filter set 40 with a KP650 red blocking filter on a Photometrics MAC 200A camera and SmartCapture V2.0 software. For all immunostainings, representative examples of at least three independent experiments are shown.

Acidic β -galactosidase staining

p53^{kd} or *PAI-1^{kd}* MEFs were infected, after 4 days plated under low density (5×10^4 cells in a 10-cm plate) and 24 h later stained overnight for senescence-associated acidic β -galactosidase as previously described²¹. Human post-senescent immortal *p53^{kd}* or *PAI-1^{kd}* BJ fibroblasts were infected, after 5 days plated under low density (1×10^5 cells in a 10-cm plate), and 48 h later stained overnight for acidic β -galactosidase as previously described²¹. Per plate, three independent groups of 300 cells were counted for SA- β -Gal staining. For all SA- β -Gal stainings, representative examples of at least two independent experiments are shown. Images were obtained using a Zeiss Axiovert 25 microscope with A-Plan 10× or LD A-plan 20× objectives on a Canon Powershot G3 14× zoom camera.

Western blotting

Selected cells were lysed in RIPA buffer (50 mM Tris at pH 8, 150 mM NaCl, 1% NP40, 0.5% deoxycholate, 0.1% SDS). 20, 40 or 80 micrograms of Proteins (20, 40 or 80 μ g) were separated by 8–12% SDS-PAGE and transferred to polyvinylidene difluoride membranes (Millipore, Billerica, MA). Western blots were probed with the indicated antibodies. For all western blots representative examples of at least two independent experiments are shown.

Coimmunoprecipitations

Total cell lysates were isolated with ELB buffer (0.25 M NaCl, 0.1% NP40, 50 mM HEPES at pH 7.3) supplemented with Complete protease inhibitors (Roche). Cytoplasmic fractions of BJ cells were isolated with nuclear and cytoplasmic extraction kit NE-PER (Pierce Biotechnology Inc., Rockford, IL) according to manufacturers' instructions. Lysates were incubated with protein-A-Sepharose beads (Amersham-Pharmacia Biotech, Piscataway, NJ) coated with anti-cyclin D1 (M20, Santa Cruz Biotechnology). Analysis of cyclin D1 or cyclin D1-associated proteins was performed by western blotting the precipitates from cytoplasmic and total lysates.

Supplementary Material

Refer to Web version on PubMed Central for supplementary material.

Acknowledgments

We would like to thank A. Visser for technical assistance, K. Berns, M. Hijmans, A. Dirac, T. Brummelkamp, R. Agami, R. van der Kammen, J. Collard and F. Scheeren for retroviral constructs, B. Weigelt for help with QRT-PCR, F. Foijer for retinoblastoma family deficient MEFs, L. Oomen and L. Brocks for help with microscopy, and R. Beijersbergen and D. Peepers for helpful discussions. This work was supported by a grant from the Dutch Cancer Society to R.B. and a grant from the National Institutes of Health (NIH; GM57242) to P.H.

References

1. Lundberg AS, Hahn WC, Gupta P, Weinberg RA. Genes involved in senescence and immortalization. *Curr. Opin. Cell Biol* 2000;12:705–709. [PubMed: 11063935]
2. Sherr CJ, McCormick F. The RB and p53 pathways in cancer. *Cancer Cell* 2002;2:103–112. [PubMed: 12204530]
3. Massague J. G1 cell-cycle control and cancer. *Nature* 2004;432:298–306. [PubMed: 15549091]
4. Pantoja C, Serrano M. Murine fibroblasts lacking p21 undergo senescence and are resistant to transformation by oncogenic Ras. *Oncogene* 1999;18:4974–4982. [PubMed: 10490832]
5. Kunz C, Pebler S, Otte J, von der Ahe D. Differential regulation of plasminogen activator and inhibitor gene transcription by the tumor suppressor p53. *Nucleic Acids Res* 1995;23:3710–3717. [PubMed: 7479001]
6. Zhao R, et al. Analysis of p53-regulated gene expression patterns using oligonucleotide arrays. *Genes Dev* 2000;14:981–993. [PubMed: 10783169]
7. Mu XC, Higgins PJ. Differential growth state-dependent regulation of plasminogen activator inhibitor type-1 expression in senescent IMR-90 human diploid fibroblasts. *J. Cell Physiol* 1995;165:647–657. [PubMed: 7593245]
8. Martens JW, et al. Aging of stromal-derived human breast fibroblasts might contribute to breast cancer progression. *Thromb. Haemost* 2003;89:393–404. [PubMed: 12574821]
9. Serrano M, Lin AW, McCurrach ME, Beach D, Lowe SW. Oncogenic ras provokes premature cell senescence associated with accumulation of p53 and p16INK4a. *Cell* 1997;88:593–602. [PubMed: 9054499]
10. De Petro G, Copeta A, Barlati S. Urokinase-type and tissue-type plasminogen activators as growth factors of human fibroblasts. *Exp. Cell Res* 1994;213:286–294. [PubMed: 8020601]
11. Brummelkamp TR, Bernards R, Agami R. Stable suppression of tumorigenicity by virus-mediated RNA interference. *Cancer Cell* 2002;2:243–247. [PubMed: 12242156]
12. Andreasen PA, Egelund R, Petersen HH. The plasminogen activation system in tumor growth, invasion, and metastasis. *Cell Mol. Life Sci* 2000;57:25–40. [PubMed: 10949579]
13. Choong PF, Nadesapillai AP. Urokinase plasminogen activator system: a multifunctional role in tumor progression and metastasis. *Clin. Orthop* 2003;415:S46–S58. [PubMed: 14600592]
14. Quelle DE, et al. Cloning and characterization of murine *p16INK4a* and *p15INK4b* genes. *Oncogene* 1995;11:635–645. [PubMed: 7651726]
15. Linardopoulos S, et al. Deletion and altered regulation of *p16INK4a* and *p15INK4b* in undifferentiated mouse skin tumors. *Cancer Res* 1995;55:5168–5172. [PubMed: 7585567]
16. Sherr CJ. Tumor surveillance via the ARF-p53 pathway. *Genes Dev* 1998;12:2984–2991. [PubMed: 9765200]
17. Cross DA, Alessi DR, Cohen P, Andjelkovich M, Hemmings BA. Inhibition of glycogen synthase kinase-3 by insulin mediated by protein kinase B. *Nature* 1995;378:785–789. [PubMed: 8524413]
18. Vivanco I, Sawyers CL. The phosphatidylinositol 3-Kinase AKT pathway in human cancer. *Nature Rev. Cancer* 2002;2:489–501. [PubMed: 12094235]
19. Diehl JA, Cheng M, Roussel MF, Sherr CJ. Glycogen synthase kinase-3 β regulates cyclin D1 proteolysis and subcellular localization. *Genes Dev* 1998;12:3499–3511. [PubMed: 9832503]
20. Chandrasekar N, et al. Downregulation of uPA inhibits migration and PI3k/Akt signaling in glioblastoma cells. *Oncogene* 2003;22:392–400. [PubMed: 12545160]
21. Dimri GP, et al. A biomarker that identifies senescent human cells in culture and in aging skin *in vivo*. *Proc. Natl Acad. Sci. USA* 1995;92:9363–9367. [PubMed: 7568133]
22. Parsons R. Human cancer, PTEN and the PI-3 kinase pathway. *Semin. Cell Dev. Biol* 2004;15:171–176. [PubMed: 15209376]
23. Radu A, Neubauer V, Akagi T, Hanafusa H, Georgescu MM. PTEN induces cell cycle arrest by decreasing the level and nuclear localization of cyclin D1. *Mol. Cell Biol* 2003;23:6139–6149. [PubMed: 12917336]

24. Dannenberg JH, van Rossum A, Schuijff L, te Riele H. Ablation of the retinoblastoma gene family deregulates G(1) control causing immortalization and increased cell turnover under growth-restricting conditions. *Genes Dev* 2000;14:3051–3064. [PubMed: 11114893]
25. Sage J, et al. Targeted disruption of the three Rb-related genes leads to loss of G(1) control and immortalization. *Genes Dev* 2000;14:3037–3050. [PubMed: 11114892]
26. Rowland BD, et al. E2F transcriptional repressor complexes are critical downstream targets of p19 (ARF)/p53-induced proliferative arrest. *Cancer Cell* 2002;2:55–65. [PubMed: 12150825]
27. West MD, Shay JW, Wright WE, Linskens MH. Altered expression of plasminogen activator and plasminogen activator inhibitor during cellular senescence. *Exp. Gerontol* 1996;31:175–193. [PubMed: 8706787]
28. Brown JP, Wei W, Sedivy JM. Bypass of senescence after disruption of *p21CIP1/WAF1* gene in normal diploid human fibroblasts. *Science* 1997;277:831–834. [PubMed: 9242615]
29. Berns K, et al. A large-scale RNAi screen in human cells identifies new components of the p53 pathway. *Nature* 2004;428:431–437. [PubMed: 15042092]
30. Chen Z, et al. Crucial role of p53-dependent cellular senescence in suppression of Pten-deficient tumorigenesis. *Nature* 2005;436:725–730. [PubMed: 16079851]
31. Tuveson DA, et al. Endogenous oncogenic K-ras(G12D) stimulates proliferation and widespread neoplastic and developmental defects. *Cancer Cell* 2004;5:375–387. [PubMed: 15093544]
32. Prendergast GC, Diamond LE, Dahl D, Cole MD. The c-myc-regulated gene *mrl* encodes plasminogen activator inhibitor 1. *Mol. Cell Biol* 1990;10:1265–1269. [PubMed: 2406566]
33. Parfyonova YV, Plekhanova OS, Tkachuk VA. Plasminogen activators in vascular remodeling and angiogenesis. *Biochemistry (Mosc)* 2002;67:119–134. [PubMed: 11841347]
34. Bissell MJ, et al. Tissue structure, nuclear organization and gene expression in normal and malignant breast. *Cancer Res* 1999;59:S1757–S1763.
35. Usher PA, et al. Expression of urokinase plasminogen activator, its receptor and type-1 inhibitor in malignant and benign prostate tissue. *Int. J. Cancer* 2005;113:870–880. [PubMed: 15515049]
36. Frandsen TL, et al. Direct evidence of the importance of stromal urokinase plasminogen activator (uPA) in the growth of an experimental human breast cancer using a combined uPA gene-disrupted and immunodeficient xenograft model. *Cancer Res* 2001;61:532–537. [PubMed: 11212246]
37. Almholt K, et al. Reduced metastasis of transgenic mammary cancer in urokinase-deficient mice. *Int. J. Cancer* 2005;113:525–532. [PubMed: 15472905]
38. Tuxhorn JA, Ayala GE, Rowley DR. Reactive stroma in prostate cancer progression. *J. Urol* 2001;166:2472–2483. [PubMed: 11696814]
39. Mueller MM, Fusenig NE. Friends or foes — bipolar effects of the tumour stroma in cancer. *Nature Rev. Cancer* 2004;4:839–849. [PubMed: 15516957]
40. Dirac AM, Bernards R. Reversal of senescence in mouse fibroblasts through lentiviral suppression of p53. *J. Biol. Chem* 2003;278:11731–11734. [PubMed: 12551891]
41. Yu JY, Taylor J, DeRuiter SL, Vojtek AB, Turner DL. Simultaneous inhibition of GSK3 α and GSK3 β using hairpin siRNA expression vectors. *Mol. Ther* 2003;7:228–236. [PubMed: 12597911]

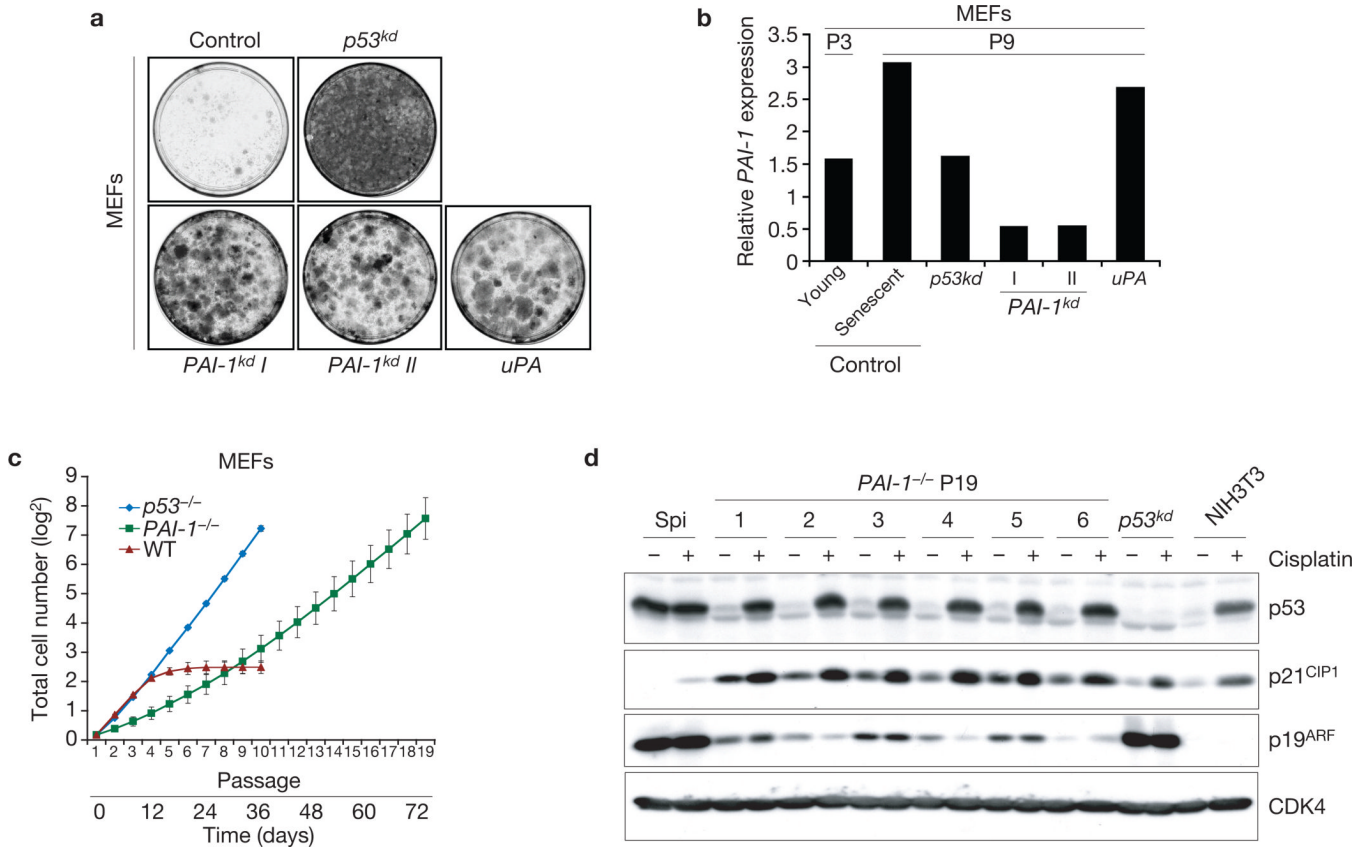


Figure 1. *PAI-1* loss induces senescence-bypass in primary mouse fibroblasts. **(a)** Colony formation assay in primary MEFs overexpressing the indicated constructs. A knockdown vector for *p53* was used as a positive control. **(b)** Relative *PAI-1* expression analysed by QRT-PCR on extracts from the indicated post-senescent polyclonal cell lines. P3 are young passage 3 and P9 are senescent passage 9 MEFs. **(c)** Growth curves of *PAI-1^{-/-}*, *p53^{-/-}* and wild-type (WT) MEFs. For each genotype the mean \pm s.d. of six independent cultures is shown. **(d)** Western blot analysis of a spontaneously immortal line (spi), six independent *PAI-1^{-/-}* passage 19 (P19), *p53^{kd}* and *p16^{INK4A}-p19^{ARF}*-deficient immortal NIH3T3 cell lines showing status of p53 and its targets p19^{ARF} and p21^{CIP1} after cisplatin-induced DNA damage. CDK4 is a loading control. Uncropped full scans are shown in the Supplementary Information.

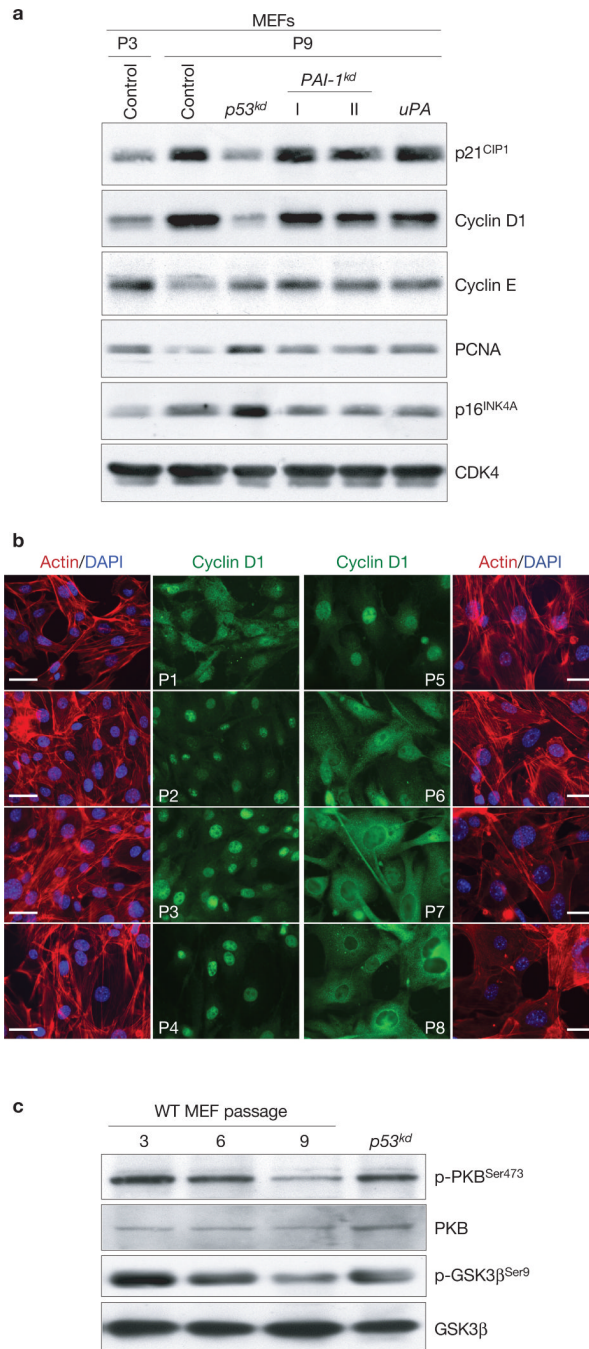
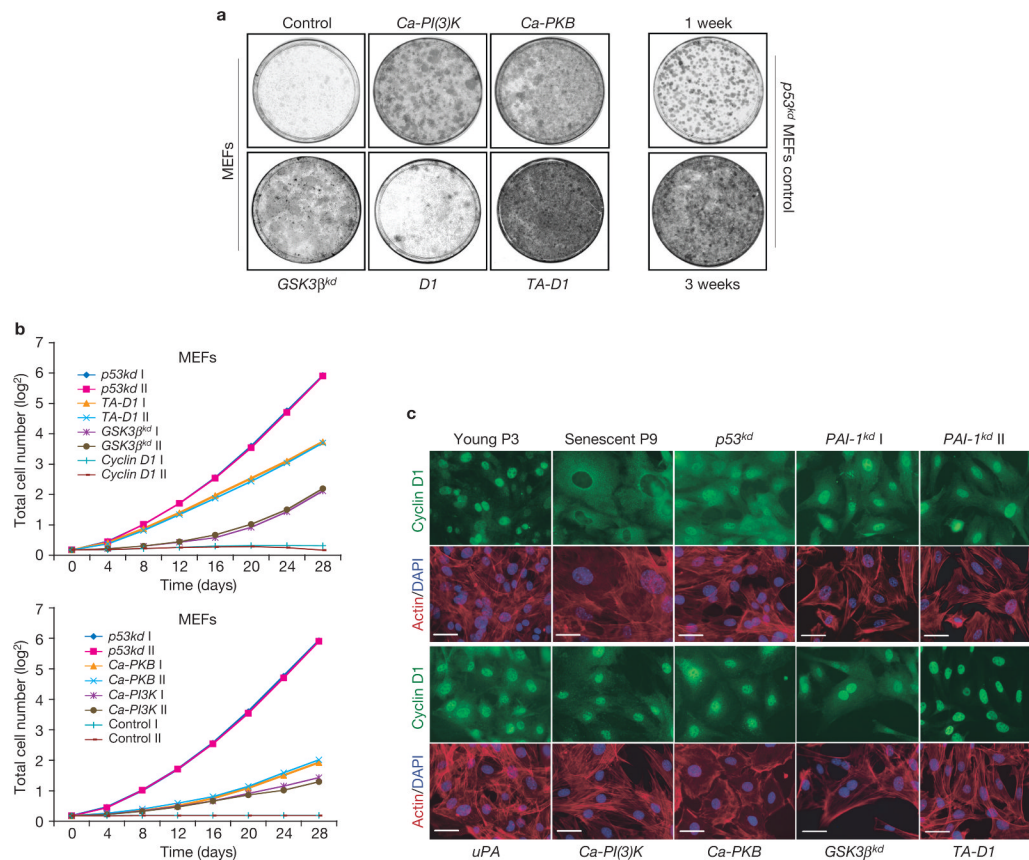


Figure 2. MEFs reduce PKB activation and exclude cyclin D1 from the nucleus during replicative senescence. **(a)** Western blot analysis of P3, P9, *p53^{kd}*, *PAI-1^{kd}* or *uPA* overexpressing MEFs for cell-cycle related proteins. PCNA and CDK4 are proliferation and loading controls, respectively. **(b)** Qualitative immunofluorescence microscopy analysis of serially passaged MEFs, (P1–P8), for cyclin D1 expression. The scale bar represents 50 μm . **(c)** Expression of phosphorylated PKB or GSK3 β related to unphosphorylated fraction of the same proteins in P3, P6 and P9 MEFs and post-senescent *p53^{kd}* cells as analysed by western blot.

**Figure 3.**

Sustained PI(3)K–PKB signalling or nuclear retention of cyclin D1 induces bypass of senescence. **(a)** Colony formation assay of primary MEFs infected with the indicated retroviral constructs. Immortalizing efficiency controls are *p53^{kd}* MEFs stained after 1 or 3 weeks. **(b)** Growth curves of various depicted immortalizing constructs versus wild-type *cyclin D1* infected MEFs. Overexpression of *p53^{kd}* or control vector are positive and negative controls, respectively. The results shown are of two independent infections per construct (I, II). **(c)** Qualitative immunofluorescence microscopy analysis for cyclin D1 of post-senescent MEFs immortalised with the indicated constructs and control P3 and P9 MEFs. The scale bar represents 50 μm.

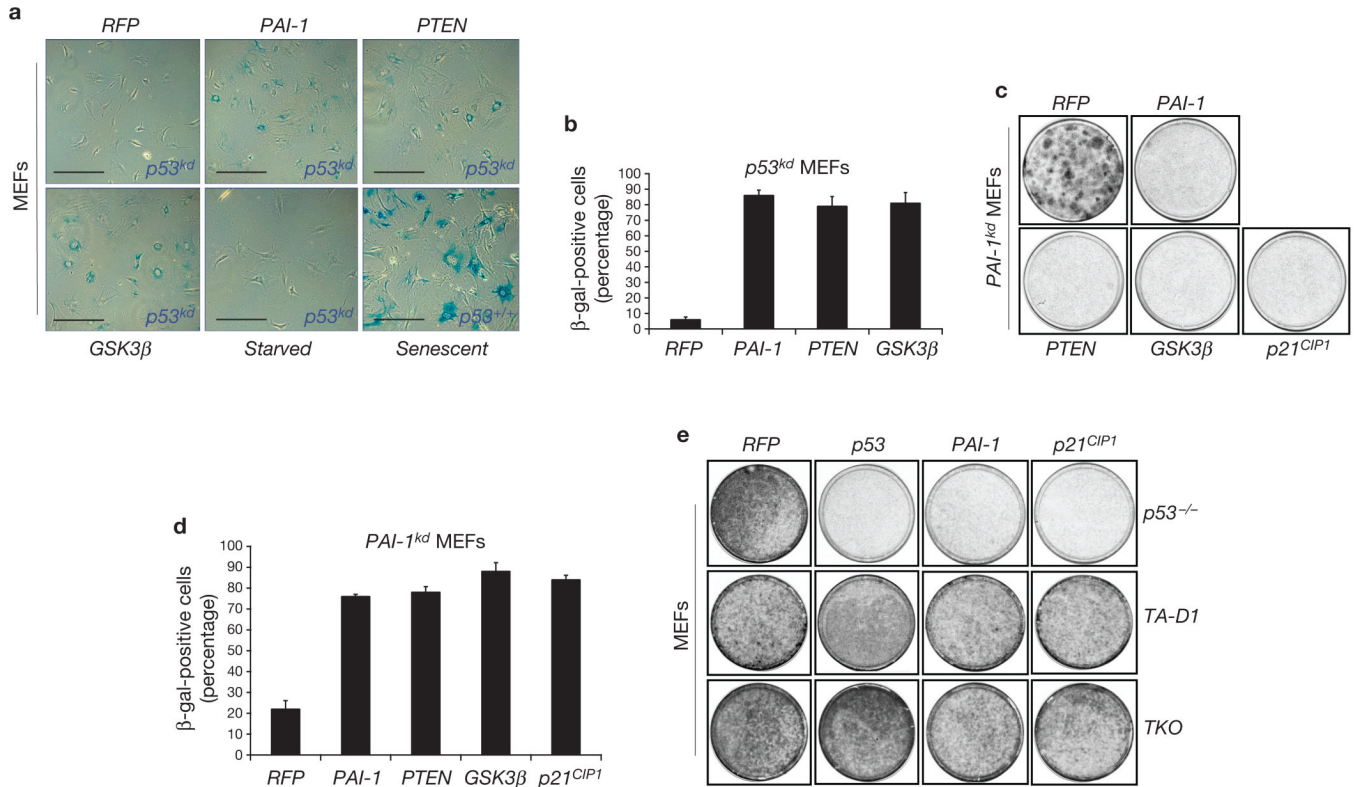


Figure 4. *PAI-1* expression is sufficient for the induction of replicative senescence. **(a)** *PAI-1*, *PTEN* or *GSK3β* overexpression induces senescence in *p53^{kd}* MEFs as indicated by staining for senescence-associated β-galactosidase (SA-β-Gal). Control cells are mock-infected, serum depleted (starved) and wild-type senescent MEFs. The scale bar represents 400 μm. **(b)** Quantification of SA-β-Gal-positive *p53^{kd}* cells after retroviral overexpression of constructs as indicated in **a**. The mean ± s.d. of three independent plates is shown. **(c)** Colony formation assay in immortal *PAI-1^{kd}* MEFs after retroviral overexpression of the indicated constructs. *p21^{CIP1}* and red fluorescent protein (*RFP*) are positive and negative controls, respectively. **(d)** Quantification of SA-β-Gal-positive *PAI-1^{kd}* MEFs after retroviral overexpression of *PAI-1*, *PTEN*, *GSK3β*, *p21^{CIP1}* or an *RFP* control. Shown is the mean ± s.d. per plate per infection. **(e)** Colony formation assay in immortal *p53^{-/-}*, *TA-D1* or *TKO* (retinoblastoma family triple knockout; *pRb^{-/-}p107^{-/-}p130^{-/-}*) fibroblasts infected with indicated retroviral overexpression constructs.

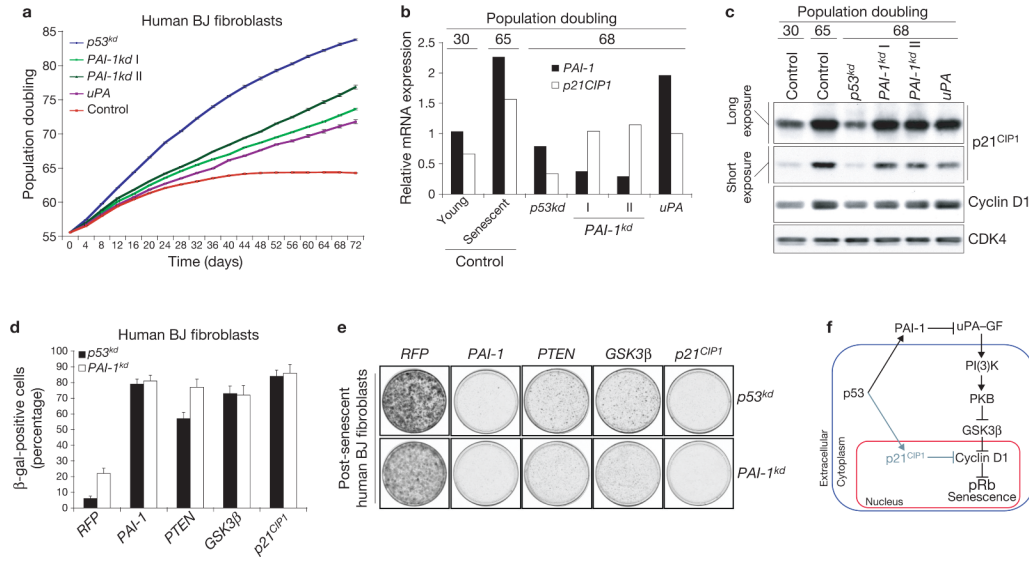


Figure 5.

PAI-1 is necessary and sufficient for senescence in human BJ fibroblasts. **(a)** Growth curves of primary human BJ fibroblasts overexpressing the indicated constructs. The mean \pm s.d. of three independent cultures per genotype is shown. **(b)** Relative *PAI-1* and *p21^{CIP1}* expression analysed by QRT-PCR on the indicated post-senescent BJ cell lines and control-infected young or senescent BJ fibroblasts. **(c)** Western blot analysis of cells from **a** for p53-target *p21^{CIP1}* and cell-cycle related protein cyclin D1. CDK4 is a loading control. **(d)** Quantification of SA- β -Gal-positive post-senescent *PAI-1^{kd}* or *p53^{kd}* BJ fibroblasts after retroviral overexpression of *PAI-1*, *PTEN*, *GSK3 β* , *p21^{CIP1}* or an RFP control. The mean \pm s.d. of three independent plates is shown. **(e)** Colony formation assay in post-senescent *p53^{kd}* or *PAI-1^{kd}* BJ fibroblasts infected with the indicated retroviral overexpression constructs. *RFP* is a negative control. **(f)** Schematic representation of a proposed model for senescence in fibroblasts. p53 induces *PAI-1* and *p21^{CIP1}* during ageing in culture. PAI-1 antagonizes uPA–GF (growth factor) signalling to cyclin D1 through PI(3)K–PKB–GSK3 β and *p21^{CIP1}* blocks cyclin D1 activity directly. The PAI-1–cyclin D1 connection is dominant over *p21^{CIP1}* activity and controls induction of the senescence response downstream of p53 and upstream of pRb.